J Solution Chem (2008) 37: 527–541
DOI 10.1007/s10953-008-9254-6

SIMEC'06

# Sorption of Lead(II) on Two Chelating Resins: From the Exchange Coefficient to the Intrinsic Complexation Constant

**Raffaela Biesuz · Giancarla Alberti · Maria Pesavento**

Received: 31 July 2007 / Accepted: 30 October 2007 / Published online: 5 February 2008

**Abstract** The sorption of inorganic lead(II) on two cationic resins containing different complexing groups, the iminodiacetic Chelex 100 and the carboxylic Amberlite CG-50, was investigated. The Gibbs-Donnan model was used to describe and predict the sorption through the determination of the intrinsic complexation constants. These quantities, even though non-thermodynamic, characterize the sorption as being independent of experimental conditions. The sorption mechanism for metals on complexing resins was also studied by adding a competitive soluble ligand that shifts the sorption curves to higher pH. The ligand competes with the resin for complexation with the metal ion. Lead(II) is strongly sorbed on Chelex 100 through the formation of two complexes in the resin phase: MHL with $\log_{10}\beta_{111i} = -0.3$ and ML with $\log_{10}\beta_{111i} = -3.7$. The presence of the competitive ligand in solution allows for the determination of a third complex. Furthermore, on Amberlite CG-50 the sorption is rather strong and involves the formation of the complex ML, in more acidic solution, with $\log_{10}\beta_{110i} = -2.0$. In the presence of the ligand PyDA, the ML(OH) complex was characterized by $\log_{10}\beta_{11-1i} = -5.6$. In all the experiments the hydrolysis reactions in the aqueous phase are considered quantitatively.

**Keywords** Sorption · Lead(II) · Chelating resins · Gibbs-Donnan model · Competition · Ligands · Ion exchange · Chelex 100 · Amberlite CG-50

## 1 Introduction

Ion-exchange and chelating resins are commonly employed for chemical separation and/or preconcentration of metal ions.

However, the choice of the best operational conditions for sorption and elution of metal ions is a problem mostly dealt with on a purely experimental basis. The main reason is that

---

R. Biesuz (✉) · G. Alberti · M. Pesavento
Dipartimento di Chimica Generale dell'Università degli Studi di Pavia, Via Taramelli 12, 27100 Pavia, Italy
e-mail: rbiesuz@unipv.it

there are no methods for the direct investigation of the resin phase and consequently the equilibria taking place inside the resin phase have not always been fully investigated.

Thermodynamic theories are mainly based on the 'Donnan type' model, handling the equilibrium as the exchange between a fixed polyelectrolyte site and a dilute electrolyte solution. They were applied to study elementary reactions, like protonation, inside the resin [1–3]. Comparisons between different models were proposed [4, 5], since often a lot of experimental data are required and the methods become inconvenient and difficult to handle.

As long as modeling of complexing reactions of heavy metals on ion exchangers is of interest, few papers can be found. A model was presented based on the formation of a surface complex [6]. A quantitative description of metal ion sorption on complexing resins can be found in Ferreira [7]. Recently, Szabadka proposed an extension of his model to these equilibria [8]. On the other hand, the exchange reactions of several metal ions on different chelating resins were investigated with the Gibbs-Donnan model. This method has been extensively described in some previous publications [9, 10]. Moreover, in this case, knowledge of sorption equilibria was applied intensively in environmental studies of the distribution of heavy metal ions in natural waters [11].

According to the proposed model, information on sorption mechanisms is quite easily achieved, working under conditions where important simplifications of the equations hold. The concepts of equilibrium chemistry are applied and, in analogy to the behavior of a soluble ligand, complexes of different compositions are found in the resin phase depending on ionic composition and the pH of the aqueous solution in contact with the resin. Satisfactory predictions of the sorption curves under different conditions were obtained.

The objective of this research was to determine the sorption equilibria of lead(II) for different complexing resins: Chelex 100 containing iminodiacetic groups and Amberlite CG-50 containing carboxylic groups. The model was validated from the comparison between the predicted and the experimental sorption curves in the case of dilute solutions of metal ions containing several complexing substances.

### 1.1 Thermodynamic Model of the Sorption of Metal Ions on Complexing Resins

The model is based on the Gibbs-Donnan description of ion-exchange resins [1, 8, 9]. The resin is represented as a solution phase, usually concentrated, separated from the external solution by an interface through which water, neutral molecules and ions can diffuse, but the active groups, permanently linked to the resin, cannot. Due to the different mobilities of ions, a potential difference is set up at the interface [12], referred to as the Donnan potential. At equilibrium, the chemical potential of each of the mobile components is the same in both phases and, for each couple of ions that can diffuse through the interface, the Donnan equilibrium is given by:

$$a_{\mathrm{A}}a_{\mathrm{C}} = \overline{a}_{\mathrm{A}}\overline{a}_{\mathrm{C}}, \qquad a_{\mathrm{C}}/a_{\mathrm{B}} = \overline{a}_{\mathrm{C}}/\overline{a}_{\mathrm{B}} \tag{1}$$

where $a$ correspond to the ion activities, A is an anion, and B and C are cations; the bars indicate the species in the resin phase. For simplicity the charges are omitted and are considered to be monovalent. The activity of an ion inside the resin cannot ever be measured, but it can be evaluated from Eq. 1 which is of basic importance for the proposed model.

In practise when solid sorbents are employed, the resin is always in excess with respect to the metal ion, which is often at trace or sub-trace levels. Under this condition, it can be assumed that mechanisms, other than formation of complexes, are negligible [9, 10] and that the concentration of active sites does not depend on complex formation. The general sorption equilibrium is:

$$\mathrm{M} + n\overline{\mathrm{H}_r\mathrm{L}} \rightleftharpoons \overline{\mathrm{MH}_p\mathrm{L}_n} + q\mathrm{H} \tag{2}$$

where M is the metal ion, $\mathrm{H}_r\mathrm{L}$ the $r$-protonated form of the active site of the resin and H is the proton. The exchange coefficient, $\beta_{1np\mathrm{ex}}$, is given by:

$$\beta_{1np\mathrm{ex}} = \frac{[\overline{\mathrm{MH}_p\mathrm{L}_n}][\mathrm{H}]^q}{[\mathrm{M}][\overline{\mathrm{H}_r\mathrm{L}}]} \tag{3}$$

The exchange coefficients depend on the concentration of the counter ion in the solution and in the resin phase whereas, to really characterize the sorption equilibria, the intrinsic complexation constants, $\beta_{1np\mathrm{i}}$, independent of the composition of the solution phase, have to be calculated. The relationship between the exchange coefficient and the intrinsic complexation constant is demonstrated to be [9, 10]:

$$\beta_{1np\mathrm{i}} = \beta_{1np\mathrm{ex}} \frac{\gamma_{\mathrm{H}}^{q}\gamma_{\mathrm{C}}^{(m-q)}}{\gamma_{\mathrm{M}}} \frac{[\mathrm{C}]^{(m-q)}}{[\overline{\mathrm{C}}]^{(m-q)}} \tag{4}$$

where $m$ is the charge of the metal and $\gamma_{\mathrm{X}}$ indicates the activity coefficient of the species X. Similar relations hold for the protonation equilibria of the resin. The exchange coefficients are evaluated from the expression for the fraction of metal ion sorbed on the resin, $f$; it is given by the following relationship:

$$f = \frac{c}{c_{\mathrm{tot}}} = \frac{[\overline{\mathrm{MH}_p\mathrm{L}_n}]w}{[\overline{\mathrm{MH}_p\mathrm{L}_n}]w + \alpha_{\mathrm{M(I)}}[\mathrm{M}]V} = \frac{1}{1 + \frac{\alpha_{\mathrm{M(I)}}[\mathrm{H}]^q V}{\beta_{1np\mathrm{ex}}[\overline{\mathrm{H}_r\mathrm{L}}]^n w}} = \frac{1}{1 + \frac{\alpha_{\mathrm{M(I)}} V}{K^* w}} \tag{5}$$

where:

| | |
|---|---|
| $w$ | is the mass of resin in grams, |
| $V$ | is the volume of the solution, |
| $c_{\mathrm{tot}}$ | is the total concentration of the metal originally present in the sample, |
| $c$ | is the concentration of the metal ion sorbed on the resin, |
| $\alpha_{\mathrm{M(I)}}$ | represents the reaction coefficient [13] of the free metal ion in the solution phase following equilibration with the resin. It is the ratio of the total metal concentration in solution (free and complexed with a ligand I present in solution), and the concentration of the free metal ion: $\alpha_{\mathrm{M(I)}} = \frac{\sum[\mathrm{MI}]}{[\mathrm{M}]}$, $\alpha_{\mathrm{M(I)}}$ is equal to one when the metal is only present as a free hydrated ion in the aqueous solution, |
| $[\overline{\mathrm{H}_r\mathrm{L}}]$ | is evaluated from the total concentration of the free active groups inside the resin ($c_{\mathrm{L}}$) and its concentration is in analytical excess with respect to the total metal ion concentration. (see below). |

Equation 5, defined for the formation of one complex, can be extended by considering the formation of other complexes, as accounted for in the last term on the r.h.s. of Eq. 5. $K^*$ represents the ratio of total metal ion in the resin phase to the free metal ion in solution. It is the partition coefficient and is given by the following relation:

$$K^* = \sum \beta_{1np\mathrm{ex}}[\overline{\mathrm{H}_r\mathrm{L}}]^n/[\mathrm{H}]^q \tag{6}$$

The summation is extended to all the complexes formed by the considered metal ion with the active groups of the resin phase.

Since $f$ is experimentally determined as is the pH of the solution, the concentration of the active sites in the resin phase and the value of $\alpha_{\mathrm{M(I)}}$ are known, the value of $\beta_{1np\mathrm{ex}}$ can be calculated from Eq. 5. The number of protons released during complexation can be estimated through a logarithmic form of Eq. 5, as previously suggested [9].

From the set of $\beta_{1np\mathrm{ex}}$ values as a function of pH, $\beta_{1np\mathrm{i}}$ can be calculated if the concentration of the counter ion in the resin phase ($[\overline{\mathrm{C}}]$) is also known (see Eq. 4).

Conversely, the intrinsic complexation constant can be used to calculate the exchange and the expected values of $f_{\mathrm{calc}}$, at any particular condition. The calculated curves of $f_{\mathrm{calc}}$ as a function of pH show graphically the ability of the model to describe the experimental sorption data. The correlation coefficient (c.c.) and the relative error, R.E. $= \sqrt{\sum(f_{\mathrm{exp}} - f_{\mathrm{calc}})^2/\sum f_{\mathrm{calc}}^2}$, are used to compare the experimental and the calculated values of $f$.

The strategy for selecting the sorption reactions is to first consider the simplest stoichiometries and reactions for those of the monomeric units in solution. This is not always enough, since often good fits are obtained considering different possible combinations.

To select the proper set, the effect of the stoichiometry on the ionic media contribution to the exchange coefficients (see Eq. 4) is considered, and consequently similar experiments are run at different I concentrations. Further indications are obtained from the evolution of profiles observed after adding a competitive ligand to the solution (see Eq. 5). In this way, it is usually possible to define the intrinsic complexation constants that will describe the sorption under any experimental conditions.

*Determination of* $\mathrm{H}_r\mathrm{L}$ *Concentration* $[\overline{\mathrm{H}_r\mathrm{L}}]$ is evaluated from the total concentration of the free active groups inside the resin ($c_{\mathrm{L}}$) according to the following relationship: $[\overline{\mathrm{H}_r\mathrm{L}}] = c_{\mathrm{L}}/\alpha_{\overline{\mathrm{H}_r\mathrm{L}}}$. The reaction coefficient of the active groups, $\alpha_{\overline{\mathrm{H}_r\mathrm{L}'}}$, is determined from the protonation coefficients of the resin.

The protonation coefficient, ($K_{ar\mathrm{ex}}$)

$$K_{ar\mathrm{ex}} = \frac{[\overline{\mathrm{H}_{r-1}\mathrm{L}}][\mathrm{H}]}{[\overline{\mathrm{H}_r\mathrm{L}}]} \tag{7}$$

is defined in analogy with the exchange coefficient, so its value depends on the counter ion concentration and the pH. For the same reason mentioned above, it is related to the intrinsic protonation constant, $K_{ar\mathrm{i}}$ [9]:

$$K_{ar\mathrm{i}} = K_{ar\mathrm{ex}} \frac{\gamma_{\mathrm{H}}\gamma_{\mathrm{C}}[\mathrm{C}]}{[\overline{\mathrm{C}}]} \tag{8}$$

It is assumed that sorbed alkali metal ions are not associated with functional groups, whereas all hydrogen ions (and metal ions) are. The association of hydrogen and metal ions and functional groups does not contribute to the internal ionic strength value. The counter ion in the resin phase depends on the amount of salt transferred. This quantity can be determined experimentally. It requires a large amount of experimental work, but it can be calculated through an iterative procedure that has been previously proposed [14].[1] It produces an estimate of $[\overline{\mathrm{H}_r\mathrm{L}}]$ and $[\overline{\mathrm{C}}]$ as a function of pH for a given counter ion concentration in solution, for the two resins.

---

[1] An algorithm incorporated in a MS-Excel spreadsheet can be acquired to the authors [14].

## 2 Experimental Section

### 2.1 Reagents

All chemicals were analytical reagent grade. Solutions were prepared with ultrapure water (Milli-Q). Chelex 100 [CAS 68954-42-7] (Bio-Rad Laboratories), with a particle size of 100–200 mesh was delivered in the sodium form. It was washed and converted into the $H^+$ form with ultrapure $HNO_3$ as previously described [9]. Amberlite CG-50 [CAS 9042-11-9] (Sigma-Aldrich) was delivered in the $H^+$ form. It was washed, cleaned and stored, as mentioned above in the case of Chelex 100 [9].

The capacity of the resins (mmole of active groups per g of dry resin) was found to be $2.0\ \text{mmol}\cdot\text{g}^{-1}$ of dry resin for Chelex 100 in $H^+$ form and $10.0\ \text{mmol}\cdot\text{g}^{-1}$ of dry resin Amberlite CG-50 that, together with the amount of water sorbed by the resins, were determined as described elsewhere [9, 10]. A lead atomic spectroscopy standard solution (Fluka) of $1000\ \text{mg}\cdot\text{L}^{-1}$ [CAS 10099-74-8] and $Pb(NO_3)_2$ [CAS 10099-74-8] Riedel De Haen were used to have the appropriate Pb(II) concentration in the solution phase.

The considered aqueous soluble complexing agents were nitrilotriacetic acid, NTA, $C_6H_9NO_6$ [CAS 139-13-9] (Fluka); pyridine dicarboxylic acid, $C_7H_5NO_4$ [CAS 499-83-2] (Merck-Schuchardt). Solutions were prepared by dissolution of the solids.

### 2.2 Apparatus

A PHM 84 Research pH meter, Radiometer Copenhagen, with an ABU 80 autoburette and a combined Orion glass electrode were used for the pH measurements. The potentiometric cell was standardized in terms of the $H^+$ concentration as previously reported [9]. A small overpressure of nitrogen was applied in the vessel that was placed in a thermostat bath at 25 °C.

A AA-6601G/GFA Shimadzu graphite furnace atomic absorption spectrophotometer with a 6100 Shimadzu autosampler for determining the concentration of Pb(II) in the case of dilute solution, with a linearity up to $10\ \mu\text{g}\cdot\text{L}^{-1}$, and $0.13\ \mu\text{g}\cdot\text{L}^{-1}$ for LOD and $0.44\ \mu\text{g}\cdot\text{L}^{-1}$ LOQ.

A Jobin Yvon ICP, equipped with an ICP JY2301 torch, a JY2900 oscillograph and an UV JY38 monochromator was used to determine the Pb(II) concentration up to $4\ \text{mg}\cdot\text{L}^{-1}$, the limits for LOD and LOQ being 0.16 and $0.76\ \text{mg}\cdot\text{L}^{-1}$, respectively.

### 2.3 Determination of the Sorption Profiles

The experimental sorption profiles are curves obtained by plotting the ratio of sorbed to total metal ion ($f$) versus pH; the procedure is described in detail elsewhere [9, 10] and is briefly reported here. A fixed volume of solution (30 mL) with a known composition and concentration of metal ion was equilibrated with a known amount of resin, gently stirred under a low $N_2$ overpressure to avoid any contact with atmospheric $CO_2$. The quantity of resin was selected to have a large excess of active groups compared to the total amount of metal ion. The pH was measured potentiometrically and adjusted with small amounts of acid or base. The equilibration time adopted for lead sorption on the resins was around 3 h as checked in preliminary experiments. The pH of the suspension was measured and recorded following equilibration; a small amount of solution (0.1–0.2 mL) was collected, diluted to 5 mL with $0.1\ \text{mol}\cdot\text{L}^{-1}$ $HNO_3$ and analyzed for the Pb(II) content. The amount of Pb(II) sorbed was calculated by difference from the total.

In some experiments, when low concentrations of Pb are considered (around $10^{-4}$ mol·L$^{-1}$), the sorption profile was also obtained in a batch mode by preparing a number of samples (10–15) with the same composition and varying only the pH of the aqueous phase. After equilibration, the resin is separated from solution, rapidly washed and the sorbed metal ion eluted and preconcentrated in 5 mL 0.1 mol·L$^{-1}$ $HNO_3$, then analyzed for the Pb(II) content.

## 3 Results and Discussion

### 3.1 Sorption of Lead(II) on Chelex 100

The sorption of lead(II) on Chelex 100 was investigated from solutions at different concentrations of $NaNO_3$, in the presence and absence of competing ligand and at different total metal concentrations. The total number of the active sites in the resin was always in excess with respect to the total amount of the metal ion, so that the total concentrations of the free active group inside the resin are independent of the metal sorption.

The sorption profiles obtained in the absence of competing ligand are reported as an example in Fig. 1. These were obtained in 0.1 and 1.0 mol·L$^{-1}$ $NaNO_3$; represented in Fig. 1 with circles and rhombuses, respectively. The points are experimental values, whereas the curves were calculated according to Eq. 5. It is evident that lead(II) is sorbed on Chelex 100 at pH higher than 1. The difference obtained at two different concentrations of $NaNO_3$ depends on the stoichiometry of the sorption reaction when $(m - q) \neq 0$ (see Eq. 4).

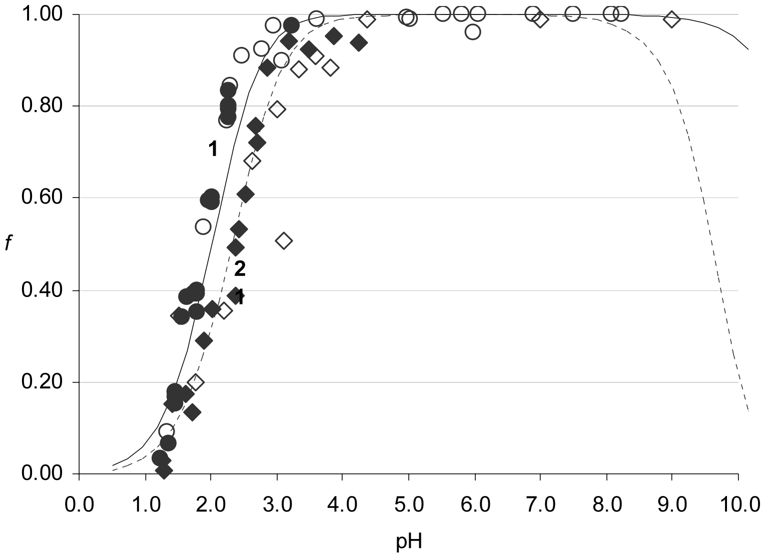

**Fig. 1** Sorption profiles of lead(II) on Chelex 100 from 0.1 mol·L$^{-1}$ $NaNO_3$ solutions: (●), $V = 30.8$ mL, $c_{Pb} = 2.03 \times 10^{-3}$ mol·L$^{-1}$ and 0.361 g of dry resin, (○), $V = 30.8$ mL, $c_{Pb} = 1.14 \times 10^{-6}$ mol·L$^{-1}$ and 0.346 g of dry resin; from 1.0 mol·L$^{-1}$ $NaNO_3$ solutions: (◆), $V = 30.8$ mL, $c_{Pb} = 1.96 \times 10^{-3}$ mol·L$^{-1}$ and 0.356 g of dry resin, (◇), $V = 30.8$ mL, $c_{Pb} = 1.21 \times 10^{-6}$ mol·L$^{-1}$ and 0.346 g of dry resin. Lines were calculated considering the formation of MHL. *Line 1* for a 0.1 mol·L$^{-1}$ $NaNO_3$ solution; *line 2* for a 1.0 mol·L$^{-1}$ $NaNO_3$ solution

**Table 1** Values of hydrolysis constants of lead extrapolated at $I \rightarrow 0$ used in calculation of $\alpha_{\mathrm{M(I)}}$ for the hydrolysis contribution referred to the reaction: $x\mathrm{Pb}^{2+} + \mathrm{H_2O} \rightleftarrows \mathrm{Pb}_x(\mathrm{OH})_y^{2x-y} + y\mathrm{H}^+$

| | $\log^*_{10}\beta_{x,y}$ | $x$ | $y$ |
|---|---|---|---|
| $\mathrm{Pb(OH)_2^0}$ | −17.1 | 1 | 2 |
| $\mathrm{Pb(OH)_3^-}$ | −28.1 | 1 | 3 |
| $\mathrm{Pb(OH)_4^{2-}}$ | −39.7 | 1 | 4 |
| $\mathrm{Pb_2(OH)^{3+}}$ | −6.4 | 2 | 1 |
| $\mathrm{Pb_3(OH)_4^{2+}}$ | −23.9 | 3 | 4 |
| $\mathrm{Pb_4(OH)_4^{4+}}$ | −20.9 | 4 | 4 |
| $\mathrm{Pb_6(OH)_8^{4+}}$ | −43.6 | 6 | 8 |
| $\mathrm{PbOH^+}$ | −7.7 | 1 | 1 |
| $\mathrm{Pb(OH)_{2(c)}}$ | −8.1 | 1 | 2 |
| $\mathrm{PbO_{(c)}}$ | −12.9 | 1 | 2 |
| $\mathrm{PbO{:}Pb(OH)_{2(c)}}$ | −26.2 | 2 | 4 |

The filled symbols represent sorption profiles when the total Pb(II), $c_{\mathrm{Pb}}$, is $\sim 2 \times 10^{-3}$ mol·L$^{-1}$, the open symbols correspond to $\sim 1 \times 10^{-6}$ mol·L$^{-1}$, (the actual concentrations values are given in the caption to Fig. 1). These series differ only in their metal contents. Since the resin is in large excess, no differences are expected for curves obtained at the two $c_{\mathrm{Pb}}$ levels.

The hydrolysis reactions and the formation of insoluble hydroxyl compounds in principle compete with the complexation reactions in the resin phase. When the higher Pb concentration was considered, the pH of the solution phase was always below pH = 4.5–5 to avoid precipitation, whereas in the case of dilute metal solutions, the pH was extended to ten without observing any precipitation. The effect of the hydrolysis competition is quantified by the reaction coefficient, $\alpha_{\mathrm{M(I)}}$, which is calculated from the total Pb(II) content, the ionic media concentration, the pH and the constants values of the several hydrolysis reactions. The "IUPAC Stability Constants Database" produced by Academic Software [15] was used for selecting the hydrolysis constants, reported in Table 1 for $I \rightarrow 0$. The values of $\alpha_{\mathrm{M(I)}}$ for hydrolysis were always calculated with the program Medusa [16].

For these series of experiments, sorption on the resin is quantitative at pH lower than four, so the exchange reaction between the metal and the resin is detected and measured when it does not depend on the hydrolysis reactions. Actually the reaction coefficient due to hydrolysis depends on the total lead concentration, because polymeric reactions are involved and consequently so does $f$ (see Eq. 5), but in 0.1 mol·L$^{-1}$ $\mathrm{NaNO_3}$ solution, with $c_{\mathrm{Pb}} \sim 2 \times 10^{-3}$ mol·L$^{-1}$, the reaction coefficient is higher than 1 at pH > 5.6 and, with $c_{\mathrm{Pb}} \sim 1 \times 10^{-6}$ mol·L$^{-1}$, at pH > 7. Consequently, for pH < 4, $\alpha_{\mathrm{M(I)}}$ is definitively equal to one for the two different metal concentrations; the profiles obtained are expected to overlap, and this agrees with the experimental findings. The sorption of Pb(II) on Chelex 100 takes place at lower pH through the reaction:

$$\mathrm{M} + \overline{\mathrm{H_2L}} \rightleftarrows \overline{\mathrm{MHL}} + \mathrm{H} \tag{9}$$

The values of the intrinsic complexation constant are reported in Table 2. For each experiment, the average values were obtained for those points with $0.2 < f_{\mathrm{exp}} < 0.8$. The standard deviation is also reported in Table 2. A higher uncertainty of the intrinsic constant is obtained at dilute metal concentrations, but $\log_{10}\beta_{111i}$ is not significantly different from the

**Table 2** Intrinsic complexation constants relative to the sorption of lead(II) on the resin, Chelex 100, obtained in solutions of different composition

| $NaNO_3$ ($mol\cdot L^{-1}$) | $c_{Pb}$ ($mol\cdot L^{-1}$) | $\log_{10}\beta_{111i}$ | Fitting parameters |
|---|---|---|---|
| 0.1 | $2.03\times10^{-3}$ | −0.24(9) | 33 objects |
| 0.1 | $1.14\times10^{-6}$ | −0.3(3) | c.c. = 0.993 |
| | | | R.E. = 0.08 |
| 1.0 | $1.96\times10^{-3}$ | −0.3(1) | 23 objects |
| 1.0 | $1.21\times10^{-6}$ | −0.3(1) | c.c. = 0.970 |
| | | | R.E. = 0.16 |

| $NaNO_3$ ($mol\cdot L^{-1}$) | $c_M, c_L$ ($mol\cdot L^{-1}$) | $\log_{10}\beta_{111i}$ | $\log_{10}\beta_{110i}$ | $\log_{10}\beta_{11\text{-}1i}$ | Fitting parameters |
|---|---|---|---|---|---|
| 0.1 | $c_{Pb}=2\times10^{-3}$<br>$c_{NTA}=5\times10^{-3}$ | −0.3 | −3.7 | −9.3 | 26 objects<br>c.c. = 0.980<br>R.E. = 0.10 |
| 0.1 | $c_{Pb}=2.20\times10^{-4}$<br>$c_{NTA}=5.4\times10^{-3}$ | | | | |
| 0.1 | $c_{Pb}=1.18\times10^{-6}$<br>$c_{NTA}=5.3\times10^{-3}$<br>$c_{EDTA}=1\times10^{-6}$ | −0.3 | −3.7 | −9.3 | 23 objects<br>c.c. = 0.936<br>R.E. = 0.27 |
| 0.1 | $c_{Pb}=1.52\times10^{-6}$<br>$c_{NTA}=5.5\times10^{-3}$<br>$c_{EDTA}=1\times10^{-6}$ | | | | |
| 1.0 | $c_{Pb}=1.8\times10^{-3}$<br>$c_{NTA}=5.5\times10^{-3}$ | −0.2 | −3.7 | −10.0 | 32 objects<br>c.c. = 0.996<br>R.E. = 0.05 |
| 1.0<br>1st repetition | $c_{Pb}=1.52\times10^{-6}$<br>$c_{NTA}=5.5\times10^{-3}$<br>$c_{EDTA}=1\times10^{-6}$ | −0.2 | −3.7 | −10.0 | 23 objects<br>c.c. = 0.936<br>R.E. = 0.27 |
| 1.0<br>2nd repetition | $c_{Pb}=1.52\times10^{-6}$<br>$c_{NTA}=5.5\times10^{-3}$<br>$c_{EDTA}=1\times10^{-6}$ | | | | |
| 0.1 | $c_{Pb}=9.81\times10^{-7}$<br>$c_{PyDA}=5.4\times10^{-3}$ | −0.3 | −3.7 | −9.3 | 12 objects<br>c.c. = 0.962<br>R.E. = 0.23 |

S.D.: standard deviation of the data used to estimate mean value of $\log_{10}\beta_{1np\mathrm{ex}}$
c.c.: the correlation coefficient of the calculated and experimental values of $f$
R.E.: the relative error

values obtained in more concentrated solutions, according to the two-tailed *t test*, assuming different variance and for the 95% confidence level.

In experiments in 1.0 mol·L$^{-1}$ $NaNO_3$ there is evidence of a second complex that is reasonably defined by:

$$M + \overline{H_2L} \rightleftarrows \overline{ML} + 2H \tag{10}$$

In Fig. 1, the calculated sorption curves are reported as continuous lines for each ionic composition. A satisfactory agreement with experimental data was found by always considering only reaction 9. The values of the intrinsic complexation constants used for the fitting, the correlation coefficients (c.c.) and the relative errors (R.E.), are reported in Table 2. Even in 1.0 mol·L$^{-1}$ $NaNO_3$ the values obtained at high and low metal concentrations can be considered to be identical at a 95% of confidence.

It is important to highlight that Pb(II) is sorbed in the same way at high and low concentrations. This was also reported in studies of other metal ions and confirms that the sorption sites are mainly homogeneous and no organic ligands are released by the complexing resin, able to compete for the sorption sites in combination with the metal. As matter of fact, it has been found that resins can release organics [17] that interfere with some detection techniques, such as GFAAS (graphite furnace atomic absorption) [18]. However, they do not seem to be able to complex lead(II) at the considered concentration level.

To investigate the sorption mechanism taking place at higher pH, it is convenient to add a soluble ligand that shifts the sorption curve to higher pH values, because it competes with the resin for complexation with the metal ion. This effect is accounted for quantitatively when the complexing properties of the competitive ligand are known accurately. In particular for Pb(II), the addition of a ligand forming known soluble complexes with the metal ion also acts to avoid the formation of insoluble products from Pb(II) hydrolysis.

In this study, the sorption mechanism of lead(II) on Chelex 100 at lower acidity was evaluated in the presence of NTA, in order to detect other possible complexes. In Fig. 2, several sorption profiles from solutions of 0.1 mol·L$^{-1}$ $NaNO_3$ containing NTA are reported. NTA was believed to be a strong ligand for competing effectively with Chelex 100. Protonation and complexation constants of NTA with lead [15], and the hydrolysis constants of Pb(II) already reported, were used for the evaluation of the side reaction coefficient of the metal ion. The sorption profile at a high metal concentration, $c_{Pb} = 2 \times 10^{-3}$ mol·L$^{-1}$ and $c_{NTA} = 5.12 \times 10^{-3}$ mol·L$^{-1}$, is reported as full squares in Fig. 2.

The calculated curve fits the experimental points only if the formation of a third complex in the resin phase, besides MHL and the already proposed ML, is considered. The dotted line is in fact calculated considering only the formation of MHL and ML. The third sorption reaction releases three protons, and the proposed sorption equilibrium is:

$$M + \overline{H_2L} + H_2O(l) \rightleftharpoons \overline{MLOH} + 3H \tag{11}$$

Also in 1.0 mol·L$^{-1}$ $NaNO_3$ solutions with high metal concentrations the sorption curve is well described considering these three complexes. The intrinsic complexation constants are reported in Table 2. The agreement of the intrinsic complexation constants found in the two experiments at different ionic compositions of the aqueous solution, is within the experimental error.

In Fig. 2, it is also reported with an asterisk within the black square, a profile obtained in a discontinuous way is described as the experimental section, where $c_{Pb} = 2.2 \times 10^{-4}$ mol·L$^{-1}$. It is not significantly different from that obtained at higher metal concentrations and confirms the good reproducibility of the resin properties.

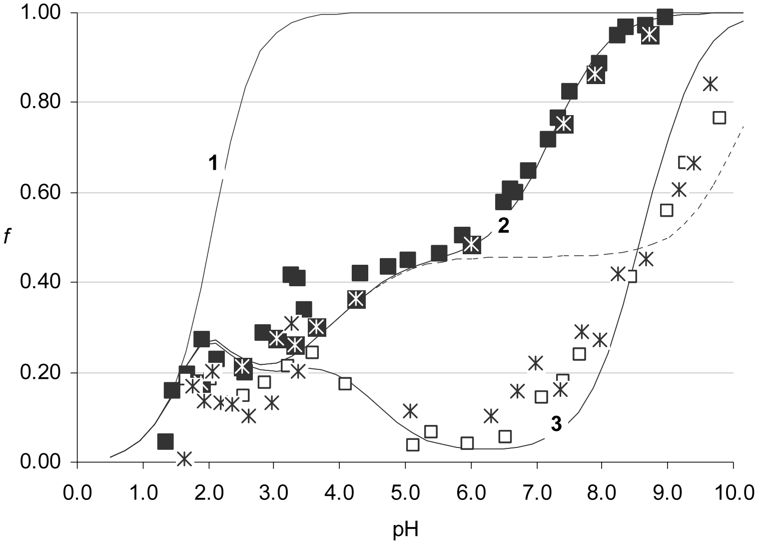

**Fig. 2** Sorption profiles of lead(II) on Chelex 100 from 0.1 mol·$L^{-1}$ $NaNO_3$ solutions containing NTA. (■), $V = 30.8$ mL, $c_{Pb} = 2 \times 10^{-3}$ mol·$L^{-1}$, $c_{NTA} = 5 \times 10^{-3}$ mol·$L^{-1}$ and 0.359 g of dry resin, (⊠), $V = 30$ mL, $c_{Pb} = 2.20 \times 10^{-4}$ mol·$L^{-1}$, $c_{NTA} = 5.4 \times 10^{-3}$ mol·$L^{-1}$ and 0.336 g of dry resin, (□), $V = 30.8$ mL, $c_{Pb} = 1.18 \times 10^{-6}$ mol·$L^{-1}$, $c_{NTA} = 5.3 \times 10^{-3}$ mol·$L^{-1}$ and 0.336 g of dry resin, (✳), $V = 30.8$ mL, $c_{Pb} = 1.52 \times 10^{-6}$ mol·$L^{-1}$, $c_{NTA} = 5.5 \times 10^{-3}$ mol·$L^{-1}$ and 0.335 g of dry resin. Continuous lines were calculated considering the formation of the complexes MHL, ML and MLOH: *line 1*, considering only hydrolysis competition; *line 2*, considering hydrolysis and NTA complexation competition; *line 3*, considering hydrolysis, NTA and EDTA complexation competition. The *dashed line* is calculated with the same condition considered for *line 2* but without the contribution of MLOH

Surprising results were obtained when the metal concentration was decreased to $10^{-6}$ mol·$L^{-1}$. In Fig. 2, the sorption profile obtained at this condition is reported with black asterisks. The unexpected behavior was confirmed by further experiments at the same condition, reported in Fig. 2 as empty squares. To explain this findings, a very strong ligand present at a trace level in NTA was assumed, whose concentration was definitively too low to be influential when $c_{Pb} = 2 \times 10^{-4}$ mol·$L^{-1}$. The same behavior was observed, always at similar total metal concentration ($\sim 10^{-6}$ mol·$L^{-1}$), in 1.0 mol·$L^{-1}$ $NaNO_3$ solutions.

Considering the presence of 0.02% EDTA in NTA, it is possible to calculate reaction coefficients that effectively describe the sorption. The curve 3 in Fig. 2 is calculated considering the complexation constants of EDTA [15], besides the hydrolysis and complexation of NTA with lead. The assumption gives a good description of experimental profiles; the same is true for curves obtained in 1.0 mol·$L^{-1}$ $NaNO_3$ solution.

The presence of this impurity was confirmed by mass tandem spectroscopy (MS-MS) on an aqueous solution of NTA. An ion with $m/z = 292.9$ Da and a fragment with $m/z = 159.9$ Da were detected and they are consistent with presence of EDTA at a ratio of roughly 1/3000 with respect to NTA. It is possible that other fragments were present, but the detected one could be responsible for the strong competition for Pb(II) complexation. The competition with the active sites in the resin is definitively much stronger than that of NTA. It was detected at very low concentration, even if in the presence of a large NTA excess, only because the metal ion was present at the same concentration level. It is important to highlight the powerful use of the Chelex 100 as probe to detect strong ligands at very low concentrations. It is the principle adopted when the authors of the present research employ this chelating resin in studies of heavy metal ion speciation in natural waters [10]. The degree of the competition with the resin by natural ligands for metal complexation allows to a description of the properties and contributions of these compounds to the effective distribution of metal species in the original sample.

The sorption at low metal concentration ($c_{\mathrm{Pb}} \sim 10^{-6}\ \mathrm{mol{\cdot}L^{-1}}$) was checked with another ligand, 2,4 pyridinedicarboxylic acid (PyDA). In this case, the sorption profile is accurately described with the three complexes in the resin phase, as found in the previous experiments with NTA, and with the reaction coefficients calculated considering, besides hydrolysis of Pb(II), the complexation of the considered ligand [15]. It is evident that, if impurities exist in PyDA, they do not show strong ligand properties.

The values of $\log_{10}\beta_{1np\mathrm{i}}$ that fit the experimental profile for the above-mentioned experiments are reported in Table 2.

### 3.2 Sorption of Lead(II) on Amberlite CG-50

The sorption of lead(II) on Amberlite CG-50 was investigated for solutions at different concentrations of $\mathrm{NaNO_3}$, with and without competing ligands and also at different total metal concentrations. In all cases the total number of active sites in the resin was in excess in comparison with the total amount of metal ion present.

Typical sorption profiles are reported in Fig. 3. They were obtained from solutions of $\mathrm{NaNO_3}$, 0.1 $\mathrm{mol{\cdot}L^{-1}}$ (full circles) and 1.0 $\mathrm{mol{\cdot}L^{-1}}$ (full rhombuses) $\mathrm{NaNO_3}$, with $c_{\mathrm{Pb}} \sim$

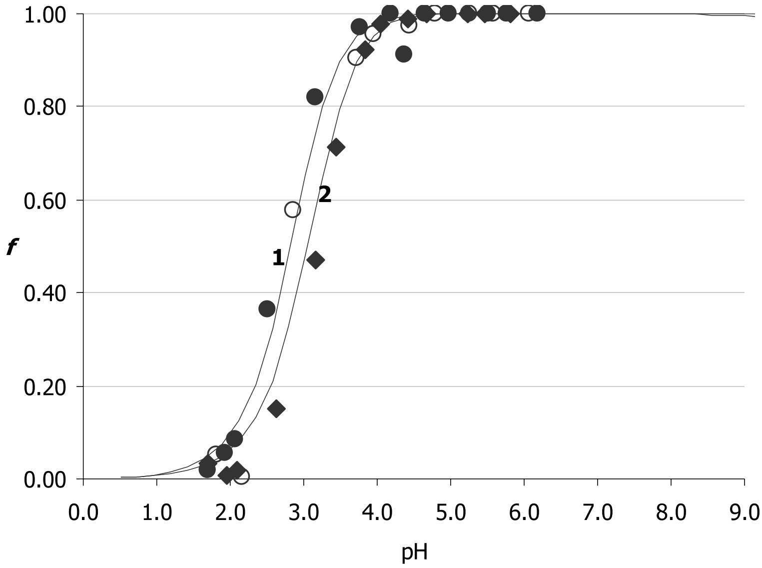

**Fig. 3** Sorption profiles of lead(II) on Amberlite CG-50 from 0.1 $\mathrm{mol{\cdot}L^{-1}}$ $\mathrm{NaNO_3}$ solutions: (●), $V = 30.8$ mL, $c_{\mathrm{Pb}} = 2.20 \times 10^{-3}\ \mathrm{mol{\cdot}L^{-1}}$ and 0.338 g of dry resin, (○), $V = 30.8$ mL, $c_{\mathrm{Pb}} = 1.04 \times 10^{-6}\ \mathrm{mol{\cdot}L^{-1}}$ and 0.366 g of dry resin; from 1.0 $\mathrm{mol{\cdot}l^{-1}}$ $\mathrm{NaNO_3}$ solutions: (◆), $V = 30.8$ mL, $c_{\mathrm{Pb}} = 2.07 \times 10^{-3}\ \mathrm{mol{\cdot}L^{-1}}$ and 0.342 g of dry resin. Continuous lines were calculated considering the formation of ML. *Line 1* for a 0.1 $\mathrm{mol{\cdot}L^{-1}}$ $\mathrm{NaNO_3}$ solution; *line 2* for a 1.0 $\mathrm{mol{\cdot}L^{-1}}$ $\mathrm{NaNO_3}$ solution

**Table 3** Intrinsic complexation constants relative to the sorption of lead(II) on the resin, Amberlite CG-50, obtained in solutions of different composition

| $NaNO_3$ ($mol \cdot L^{-1}$) | $c_{Pb}$ ($mol \cdot L^{-1}$) | $\log_{10} \beta_{110i}$ | Fitting parameters |
|---|---|---|---|
| 0.1 | $2.03 \times 10^{-3}$ | $-1.8(3)$ | 23 objects |
| 0.1 | $1.04 \times 10^{-6}$ | $-2.0(3)$ | c.c. = 0.994 |
| | | | R.E. = 0.05 |
| 1.0 | $2.07 \times 10^{-3}$ | $-2.0(3)$ | 13 objects |
| | | | c.c. = 0.999 |
| | | | R.E. = 0.03 |

| $NaNO_3$ ($mol \cdot L^{-1}$) | $c_{Pb}$, $c_L$ ($mol \cdot L^{-1}$) | $\log_{10} \beta_{110i}$ | $\log_{10} \beta_{11\text{-}1i}$ | Fitting parameters |
|---|---|---|---|---|
| 0.1 | $c_{Pb} = 2.10 \times 10^{-3}$,<br>$c_{NTA} = 5.5 \times 10^{-3}$ | $-1.8$ | $-5.6$ | 17 objects<br>c.c. = 0.92<br>R.E. = 0.4 |
| 0.1 | $c_{Pb} = 9.4 \times 10^{-7}$, $c_{NTA} = 5.2 \times 10^{-3}$,<br>$c_{EDTA} = 7 \times 10^{-7}$ | $-1.8$ | $-5.6$ | 22 objects<br>c.c. = 0.89<br>R.E. = 0.6 |
| 0.1 | $c_{Pb} = 7.7 \times 0^{-7}$, $c_{PyDA} = 5.0 \times 10^{-3}$ | | | 28 objects |
| | | $-1.8$ | $-5.8$ | c.c. = 0.984 |
| 0.1 | $c_{Pb} = 1.1 \times 10^{-6}$, $c_{PyDA} = 4.7 \times 10^{-3}$ | | | R.E. = 0.15 |

S.D.: standard deviation of the data used to estimate the mean value of $\log_{10} \beta_{1np\text{ex}}$
c.c.: the correlation coefficient of the calculated and experimental values of $f$
R.E.: the relative error

$2 \times 10^{-3}$ $mol \cdot L^{-1}$. A profile obtained with $c_{Pb} \sim 1 \times 10^{-6}$ $mol \cdot L^{-1}$ in 0.1 $mol \cdot L^{-1}$ $NaNO_3$ is reported with open circles.

From the experimental points in Fig. 3 with $0.2 < f < 0.8$, the following sorption reaction was found to take place, involving the release of one proton:

$$\mathrm{M} + \overline{\mathrm{HL}} \rightleftharpoons \overline{\mathrm{ML}} + \mathrm{H} \tag{12}$$

The intrinsic complexation constants of the sorption equilibrium are reported in Table 3, for each experimental condition. They can not be considered different at the 95% of confidence level.

The [HL] as a function of pH was evaluated as previously described. The values of $\alpha_{M(I)}$ at each pH were calculated using the computer program Medusa [16], considering the hydrolysis reactions of lead(II) as described for the sorption on Chelex 100.

In the case of 0.1 $mol \cdot L^{-1}$ $NaNO_3$, this complex provides a description of the sorption profile, while in 1.0 $mol \cdot L^{-1}$ $NaNO_3$ there is evidence of a second complex.

The effect is the same with the two resins; it depends on the increase of the counter ion concentration that makes the exchange coefficient smaller. In fact, for reactions with $(m - q) > 0$, increasing the counter ion concentration, see Eq. 4, decreases the value of $\beta_{1np\text{ex}}$. For instance, at pH = 3.95, with Amberlite CG-50, in 0.1 and 1.0 $mol \cdot L^{-1}$ $NaNO_3$

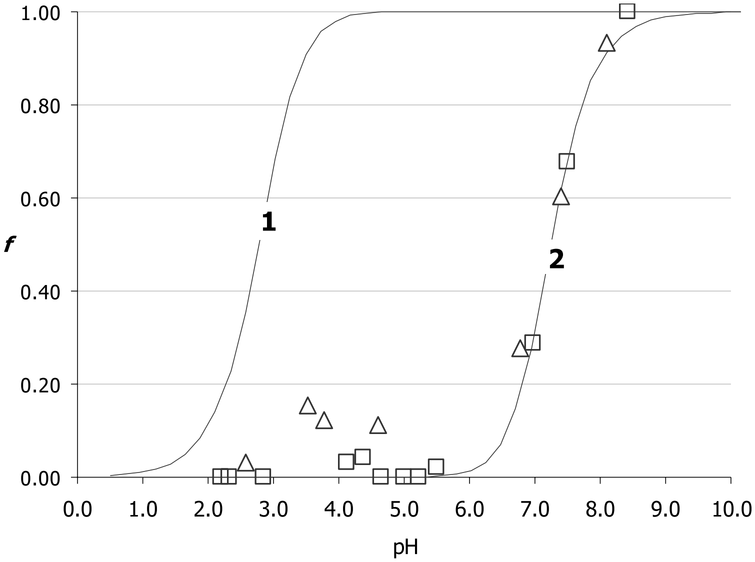

**Fig. 4** Sorption profiles of lead(II) on Amberlite CG-50 from 0.1 mol·L$^{-1}$ NaNO$_3$ solutions containing PyDA. (△), $V = 30.8$ mL, $c_{\text{Pb}} = 7.7 \times 10^{-7}$ mol·L$^{-1}$, $c_{\text{NTA}} = 5.0 \times 10^{-3}$ mol·L$^{-1}$ and 0.355 g of dry resin, (□), $V = 30.8$ mL, $c_{\text{Pb}} = 1.10 \times 10^{-6}$ mol·L$^{-1}$, $c_{\text{NTA}} = 4.7 \times 10^{-3}$ mol·L$^{-1}$ and 0.363 g of dry resin. Continuous lines were calculated considering the formation of the complexes ML and MLOH. *Line 1* considering only hydrolysis; *line 2* considering hydrolysis and PyDA complexation competition

solutions the counter ion concentration in the resin phase is estimated to be 0.382 and 1.51, respectively. It means that for $\log_{10}\beta_{110i} = -1.83$, $\log_{10}\beta_{110\text{ex}}$ is $-1.47$ in 0.1 mol·L$^{-1}$ NaNO$_3$ solution, whereas it is $-2.06$ in 1.0 mol·L$^{-1}$ NaNO$_3$. Indeed the curves are shifted to higher pH with increasing NaNO$_3$ concentration, and in order to describe the profile in 1.0 mol·L$^{-1}$ NaNO$_3$ solution, the presence of another complex must be assumed.

The value of the intrinsic complexation constant of the second complex was estimated to be roughly $\log_{10}\beta_{11\text{-}1i} \sim 5.5$, according to the exchange reaction:

$$\text{M} + \overline{\text{HL}} + \text{H}_2\text{O(l)} \rightleftharpoons \overline{\text{MLOH}} + 2\text{H} \tag{13}$$

The calculated curves are shown in Fig. 3 as continuous lines 1 and 2 for 0.1 and 1.0 mol·L$^{-1}$ NaNO$_3$, respectively. The agreement between the observed and calculated values is good and it can also be seen from the correlation coefficient and the relative error reported in Table 3.

Also in the case of Amberlite CG-50, the sorption profile is independent of the metal ion concentration. The values of the intrinsic complexation constants can to be considered equal to those obtained at higher metal ion concentrations, within experimental error at the 95% confidence level, as reported in Table 3.

NTA was considered, also in this case, to be a good competitor for lead sorption on Amberlite CG-50. Its effectiveness was evaluated in terms of $\alpha_{\text{M(I)}}$, as in the case of Chelex 100.

The second complex MLOH was needed to describe the experimental sorption profile and its stoichiometry was confirmed. No other complex between Amberlite CG-50 and lead(II) was identified. In Table 3 the values of the intrinsic complexation constants used to fit the experimental profiles are reported.

Also in this case, for the experiment at low metal ion concentration, a strong competition was observed, again consistent with the presence of a trace of EDTA. In both cases, at low and high lead(II) concentrations, a poorer fit was observed from pH = 4 to 6 whereas it is satisfactory at lower and higher acidity. Further investigations are needed to clarify sorption within this pH interval.

In Fig. 4 the sorption profiles obtained at low metal concentrations are reported, using 2,4-pyridinedicarboxylic acid as the competitive ligand in two different experiments. The continuous curve 1 is the calculated one without considering the contribution of the ligand. Curve 2 is calculated considering the already identified complexes and the contribution to $\alpha_{\mathrm{M(I)}}$, besides hydrolysis of Pb(II), of the formation constants of PyDA already used in the case of sorption on Chelex 100. The agreement between $f_{\mathrm{exp}}$ and $f_{\mathrm{calc}}$ was good, as seen also from the results reported in Table 3.

## 4 Conclusion

Lead(II) is strongly sorbed by both the considered complexing resins, Chelex 100 and Amberlite CG-50. Strong complexes are formed in the resin phase between lead(II) and the active groups present in the resin, the iminodiacetic and carboxylic groups, respectively. In both cases different complexes were detected, whose formation made it possible to predict the sorption curves over wide pH ranges. The intrinsic complexation constants characterize the sorption equilibrium, and allow the evaluation of the conditional exchange coefficients at different conditions.

It should be noticed that at least for 1:1 complexes the intrinsic complexation constants are expected to be not so different from the complexation constant of a proper monomeric unit, soluble in water [9, 10]. In the case of Chelex 100, a good correlation was already found with the complexation of methyliminodiacetic acid. Actually, considering the values reported by Napoli [19] and considering that the relation between the complexation constant and the reported formation constant is: $\log_{10}\beta_{110} = \log_{10}\beta_{\mathrm{PbL}} - \log_{10}\beta_{\mathrm{a2}}$ and $\log_{10}\beta_{111} = \log_{10}\beta_{\mathrm{PbHL}} - \log_{10}\beta_{\mathrm{a2}}$, where $\beta_{\mathrm{a2}}$ is the second overall protonation constant of methyliminodiacetic acid, i.e., $\log_{10}\beta_{\mathrm{a2}} = \log_{10}K_{\mathrm{a1}} + \log_{10}K_{\mathrm{a2}}$, the calculated value of $\log_{10}\beta_{110} = -3.83$ and also $\log_{10}\beta_{111} = -0.2$ are in very good agreement with our findings.

In the case of Amberlite CG-50, the monomeric unit used for comparison could simply be acetic acid. As long as $\log_{10}\beta_{110i}$ is concerned, the agreement was satisfactory. From the data of Veter and Romagnoli [20], an extrapolated value of $\log_{10}\beta_{110} = -2.0$ was obtained. There was no evidence in solution of the second complex identified with Amberlite CG-50.

The sorption mechanism was confirmed at high and low metal concentrations, for Chelex 100 and Amberlite CG-50, respectively. This is of importance when these sorbents are used for treating natural waters where heavy metal ions are definitively at trace levels. Moreover, the same sorption mechanisms were found by employing different competing ligands (NTA and PyDA). It is evidence that the complexation between the active site and the metal ion satisfactory describes the reactions in the resin phase.

When NTA was employed as competitor ligand and the metal ion was at low levels, it was possible to identify a trace of a strong ligand in NTA, probably EDTA, as indicated also from a MS analysis. This impurity is not released by the resins since the same effect was found for the two different resins, but not with PyDA.

**Acknowledgements** The present research was partially supported by PRIN 2005 Development of analytical methods for the characterization of environmental and food matrixes of MIUR of Italian Republic.

## References

1. Merle, Y., Marinsky, J.: Gel speciation studies I—The intrinsic dissociation constant of weakly acidic cation-exchange gels. Talanta **31**, 199–204 (1984)
2. Szabadka, Ö: Studies on chelating resins I—General equation for the calculation of the protonation constants of chelating resins. Talanta **29**, 179–181 (1982)
3. Högfeldt, E., Miyajima, T., Muhammed, M.: On protonation equilibria of Sephadex C-25 and C-50. Talanta **36**, 409–412 (1989)
4. Högfeldt, E., Szabadka, Ö., Marton, A., Varga, E.: Description of the protonation equilibria of complex forming resins by the Donnan and by the site interaction models: A comparison of the calculation methods. React. Funct. Polym. **38**, 113–126 (1998)
5. Biesuz, R., Zagorodni, A., Muhammed, M.: Estimation of deprotonation coefficients for chelating ion exchange resins. Comparison of different thermodynamic model. J. Phys. Chem. B **105**, 4751–4726 (2001)
6. Stohr, C., Horst, J., Holl, W.H.: Application of the surface complex formation model to ion exchange equilibria Part V. Adsorption of heavy metal salts onto weakly basic anion exchangers. React. Funct. Polym. **49**, 117–132 (2001)
7. Ferreira, L.M., Loureiro, J.M., Rodrigues, A.E.: Sorption of metals by an amidoxime chelating resin. Part I: equilibrium. Sep. Sci. Technol. **33**, 1585–1604 (1998)
8. Szabadka, Ö., Varga, E., Nagy, L.: Determination of protonation- and metal complex stability constants for a chelating monomer and its immobilized in polymer resin. Talanta **59**, 1081–1088 (2003)
9. Pesavento, M., Biesuz, R.: Characterisation and application of chelating resins as chemical reagents for metal ions, based on Gibbs-Donnan model. React. Funct. Polym. **36**, 135–147 (1998)
10. Biesuz, R., Pesavento, M., Alberti, G., Dalla Riva, F.: Investigation of sorption equilibria of Mn(II), Cu(II) and Cd(II) on a carboxylic resin by the Gibbs-Donnan model. Talanta **55**, 541–550 (2001)
11. Pesavento, M., Biesuz, R., Baffi, F., Gnecco, C.: Determination of metal ions concentration and speciation in seawater by titration with an iminodiacetic resin. Anal. Chim. Acta **401**, 265–276 (1999)
12. Helfferich, F.: Ion Exchange. McGraw-Hill, New York (1962)
13. Ringbon, A., Still, E.: The calculation and use of $\alpha$ coefficients. Anal. Chim. Acta **59**, 143–146 (1972)
14. Pesavento, M., Biesuz, R., Alberti, G., Dalla Riva, F.: Evaluation of the sorption of metal ions on a complexing resin in contact with different solutions based on the Gibbs Donnan model. React. Funct. Polym. **46/3**, 233–246 (2001)
15. Academic Software: IUPAC Stability Constants Database (scdbase@acadsoft.co.uk) (2001)
16. Puigdomenech, I.: MEDUSA: Make Equilibrium Diagram using Sophisticated Algorithms. Windows program, Stockholm, Version 21, Aug. 2001
17. Botta, D., Mantica, E.: Micropollutants migration from ion-exchange resins into water. Water Res. **33**, 1054–1064 (1999)
18. Baffi, F., Cardinale, A.M., Buzzone, R.: Preconcentration of chromium, copper and manganese from sea water on pretreated solid materials for determination by atomic absorption spectroscopy. Anal. Chim. Acta **270**, 79–86 (1992)
19. Napoli, A.: Lead(II) complexes of some $N$-substituted iminodiacetic acid. J. Coord. Chem. **14**, 127–131 (1985)
20. Vetere, V.F., Romagnoli, R.: Study of complexation equilibria using polarized metallic electrodes. Analyst **116**, 937–940 (1991)